Molecular Structure of Heterobimetallic μ-η^2-(C,C)-Ketene Complexes†

Munetaka Akita,* Atsuo Kondoh, and Yoshihiko Moro-oka*
Research Laboratory of Resources Utilization, Tokyo Institute of Technology, 4259 Nagatsuta, Midori-ku, Yokohama 227, Japan

---

Molecular structures of the first examples of heterobimetallic μ-η^2-(C,C)-ketene complexes, $[(OC)_2(cp)Fe(CH_2CO)Ni(cp)(CO)]$ (**1**) and $[(OC)_2(cp)Fe(CH_2CO)Mn(CO)_5]$ (**2**) (cp = η^5-C_5H_5), have been determined by single-crystal *X*-ray diffraction studies. They comprise 1,4-dimetalla-2-butanones (M–CH_2CO–M′) with significant contribution from an oxycarbene structure [M–CH_2C(O^-)=M'^+] and a π-complex resonance form {M^+[CH_2=C(O^-)–M]} in accord with previously reported spectroscopic studies.

We have been studying the reactivities of bridging ketene ligands (1-oxoethane-1,2-diyl) on polymetallic complexes as a model for surface-bound ketene species [1,2] which are recognized as one of the possible origins of oxygenated compounds in catalytic hydrogenation of carbon monoxide. Spectroscopic,[1] particularly i.r., studies of μ-ketene complexes [1,4-dimetalla-2-butanones (**A**)] reveal the significant contribution of the π-complex form (**C**) in addition to the oxycarbene structure (**B**) which is well established for mononuclear acyl metal complexes.[3] The contributors (**B**) and (**C**) arise from back donation of *d* electrons from M and M′ [M′ = $Fe(cp)(CO)_2$ where cp = η^5-C_5H_5] to the bridging ketene ligand, respectively, and the latter is the so-called β effect.[4] Here we report the results of structure determinations of the first examples of heterobimetallic μ-η^2-(C,C)-ketene complexes, $[(OC)_2(cp)Fe(CH_2CO)Ni(cp)(CO)]$ (**1**) and $[(OC)_2(cp)Fe(CH_2CO)Mn(CO)_5]$ (**2**), by *X*-ray diffraction studies. The results obtained also confirm the co-operative metal-to-ligand back donation represented above.

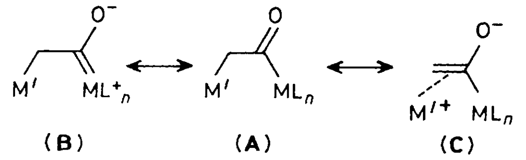

(B) (A) (C)

Experimental

The synthesis and spectroscopic characterization of complexes (**1**) and (**2**) were reported in our previous paper.[1d]

Structure Determinations.—Diffraction measurements were made on a Rigaku AFC-5 automated four-circle diffractometer by using graphite-monochromated Mo-K_α radiation (λ = 0.710 68 Å). The unit cell was determined and refined by a least-squares method using 20 independent reflections with $25 < 2\theta < 30°$. Data were collected over $2 < 2\theta < 60°$ with the ω—2θ scan technique, and three standard reflections were monitored every 100 measurements. Crystal data, data-collection parameters, and results of the analyses are listed in Table 1. Neutral scattering factors were obtained from the standard sources.[5] Data were corrected for Lorentz and polarization effects but not for absorption. Computation used the R-CRYSTAN structure-solving program system obtained from the Rigaku Corp. Full-matrix least-squares refinements minimized the function $[\Sigma w(|F_o| - |F_c|)^2/\Sigma w|F_o|^2]^{\frac{1}{2}}$ where $w = 1/[\sigma(F_o)^2 + (pF_o)^2]$, the parameter *p* being automatically optimized.

Table 1. Crystallographic data

Compound	(**1**)	(**2**)
Formula	$C_{15}H_{12}FeNiO_4$	$C_{14}H_7FeMnO_8$
Crystal system	Orthorhombic	Monoclinic
Space group	*Pbca*	$P2_1/c$
a/Å	18.886 1(52)	18.421 7(17)
b/Å	20.449 2(27)	6.870 0(16)
c/Å	7.463 3(8)	12.229 3(14)
β/°		92.853(8)
U/Å^3	2 882.39(93)	1 545.78(42)
M	370.82	414.00
Z	8	4
D_c/g cm^{-3}	1.71	1.78
Crystal size	0.3 × 0.2 × 0.4	0.2 × 0.1 × 0.3
No. of unique data [F > $3\sigma(F)$]	2 835	3 001
R	7.41	5.03
R'	8.56	3.10

$R = \Sigma(|F_o| - |F_c|)/\Sigma|F_o|$, $R' = [\Sigma w(|F_o| - |F_c|)^2/\Sigma w|F_o|^2]^{\frac{1}{2}}$.

Complexes (**1**) and (**2**) crystallized in the orthorhombic (*Pbca*) and monoclinic systems ($P2_1/_c$), respectively. The positions of the metal atoms (Fe, Ni, and Mn) were located by the direct method. Subsequent Fourier difference maps revealed the positions of all the other atoms. All non-hydrogen atoms were refined with anisotropic thermal parameters and hydrogen atoms with isotropic thermal parameters. The positional parameters and selected bond lengths and angles are listed in Tables 2—5.

Additional material available from the Cambridge Crystallographic Data Centre comprises H-atom co-ordinates, thermal parameters, and remaining bond lengths and angles.

Results and Discussion

Perspective views of complexes (**1**) and (**2**) (ORTEP drawings at 50% probability) are reproduced in Figures 1 and 2. The overall structures are primarily 1,4-dimetalla-2-butanones. As expected

---

† *Supplementary data available:* see Instructions for Authors, *J. Chem. Soc., Dalton Trans.*, 1989, Issue 1, pp. xvii—xx.

Table 2. Positional parameters for non-hydrogen atoms of complex (**1**)

Atom*	*x*	*y*	*z*
CPFE	0.408 79	0.133 28	0.331 34
CPNI	0.074 64	0.153 16	0.682 78
Fe	0.355 25(3)	0.095 62(3)	0.488 28(10)
Ni	0.145 37(2)	0.153 86(3)	0.526 02(9)
C(11)	0.450 14(38)	0.145 87(50)	0.447 14(117)
C(12)	0.448 70(43)	0.088 62(47)	0.340 35(129)
C(13)	0.392 54(53)	0.093 51(53)	0.224 35(106)
C(14)	0.357 40(38)	0.153 49(41)	0.255 97(104)
C(15)	0.395 16(38)	0.184 90(40)	0.388 87(120)
C(16)	0.287 07(31)	0.037 81(31)	0.450 63(84)
C(17)	0.387 25(29)	0.051 70(29)	0.674 45(90)
C(21)	0.115 52(32)	0.176 92(32)	0.787 20(77)
C(22)	0.102 07(40)	0.108 14(34)	0.757 06(102)
C(23)	0.052 78(35)	0.102 53(38)	0.625 52(101)
C(24)	0.032 58(32)	0.166 98(40)	0.571 93(101)
C(25)	0.070 26(34)	0.211 22(32)	0.672 20(87)
C(26)	0.166 78(34)	0.132 79(29)	0.308 45(83)
C(1)	0.290 84(29)	0.148 66(29)	0.663 20(74)
C(2)	0.239 07(29)	0.189 95(25)	0.565 79(72)
O(11)	0.245 00(25)	−0.000 60(25)	0.427 94(81)
O(12)	0.408 58(23)	0.022 01(23)	0.791 64(65)
O(21)	0.179 26(29)	0.116 66(26)	0.165 25(62)
O(1)	0.240 54(19)	0.244 80(20)	0.514 57(60)

* CPFE is the centroid of C(11)—C(15), CPNI that of C(21)–C(25).

Table 3. Selected bond lengths (Å) and angles (°) for complex (**1**)

C–C(cp)$_{av.}$(Fe)	1.393	Fe–C(cp)$_{av.}$	2.138
Fe–CPFE	1.728	Fe–C(1)	2.088(6)
Fe–C(16)	1.770(6)	Fe–C(17)	1.761(6)
C(16)–O(11)	1.130(8)	C17–O(12)	1.138(8)
C–C(cp)$_{av.}$(Ni)	1.401	Ni–C(cp)$_{av.}$	2.095
Ni–CPNI	1.776	Ni–C(2)	1.940(6)
Ni–C(26)	1.728(6)	C(26)–O(21)	1.143(8)
C(1)–C(2)	1.482(8)	C(1)–H(1A)	0.850(72)
C(1)–H(1B)	0.983(75)	C(2)–O(1)	1.205(7)
C–C–C(cp)$_{av.}$(Fe)	107.98	CP–Fe–C(1)	122.21(17)
CP–Fe–C(16)	127.98(21)	CP–Fe–C(17)	124.13(19)
C1–Fe–C(6)	91.28(26)	C(1)–Fe–C(17)	88.37(25)
C(16)–Fe–C(17)	91.97(28)	Fe–C(16)–O(11)	177.85(57)
Fe–C(17)–O(21)	178.11(61)	C–C–C(cp)$_{av.}$(Ni)	107.99
CP–Ni–C(2)	126.04(17)	CP–Ni–C(26)	142.48(21)
C(2)–Ni–C(26)	91.44(27)	Ni–C(26)–O(21)	177.23(63)
Fe–C(1)–C(2)	111.93(37)	Fe–C(1)–H(1A)	108.68(487)
Fe–C(1)–H(1B)	103.68(408)	C(2)–C(1)–H(1A)	102.41(487)
C(2)–C(1)–H(1B)	108.03(422)	H(1A)–C(1)–H(1B)	122.24(677)
C(1)–C(2)–Ni	117.38(39)	C(1)–C(2)–O(1)	124.57(52)
Ni–C(2)–O(1)	118.01(42)		

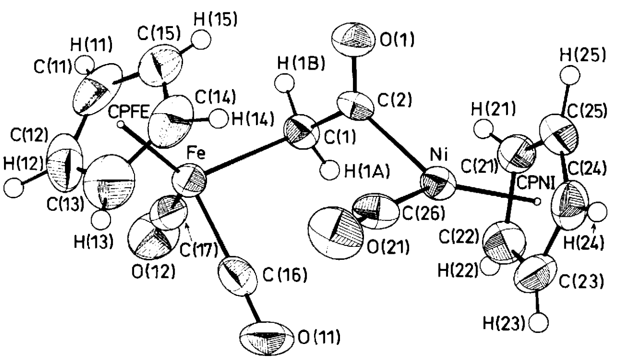

Figure 1. Molecular structure of [(OC)$_2$(cp)Fe(CH$_2$CO)Ni(cp)(CO)] (**1**) showing 50% probability thermal ellipsoids

Table 4. Positional parameters for non-hydrogen atoms of complex (**2**)

Atom*	*x*	*y*	*z*
CP	0.913 67	0.089 42	0.189 46
Fe	0.869 09(2)	0.305 79(7)	0.160 69(5)
Mn	0.626 74(2)	0.525 95(9)	0.133 95(5)
C(11)	0.970 14(22)	0.167 83(74)	0.177 51(50)
C(12)	0.935 75(25)	0.158 84(71)	0.276 08(41)
C(13)	0.870 13(25)	0.048 90(68)	0.255 26(43)
C(14)	0.865 90(23)	−0.001 00(65)	0.145 61(44)
C(15)	0.926 41(23)	0.072 51(66)	0.092 83(41)
C(16)	0.900 62(18)	0.487 82(62)	0.074 32(32)
C(17)	0.840 22(20)	0.468 09(66)	0.259 08(34)
C(1)	0.769 54(19)	0.298 86(65)	0.072 38(35)
C(2)	0.732 22(19)	0.490 50(66)	0.064 40(31)
C(21)	0.667 81(22)	0.749 68(65)	0.193 82(35)
C(22)	0.605 43(20)	0.655 32(68)	0.005 62(35)
C(23)	0.597 52(19)	0.293 18(68)	0.066 70(32)
C(24)	0.659 77(20)	0.389 35(63)	0.256 29(35)
C(25)	0.537 52(22)	0.569 69(62)	0.191 07(34)
O(11)	0.925 60(15)	0.604 34(44)	0.019 40(23)
O(12)	0.825 61(16)	0.574 36(50)	0.328 50(25)
O(1)	0.757 81(15)	0.627 55(47)	0.017 26(26)
O(21)	0.693 47(18)	0.888 87(49)	0.227 71(29)
O(22)	0.594 45(16)	0.738 51(50)	−0.074 99(25)
O(23)	0.578 78(16)	0.153 13(47)	0.025 90(28)
O(24)	0.679 31(15)	0.304 59(52)	0.332 51(23)
O(25)	0.482 24(15)	0.597 44(52)	0.225 33(28)

* CP is the centroid of C(11)–C(15).

Table 5. Selected bond lengths (Å) and angles (°) for complex (**2**)

C–C(cp)$_{av.}$	1.411	Fe–C(cp)$_{av.}$	2.103
Fe–CP	1.726	Fe–C(1)	2.082(4)
Fe–C(16)	1.754(4)	Fe–C(17)	1.743(4)
C(16)–O(11)	1.155(5)	C(17)–O(12)	1.161(5)
Mn–C(2)	2.173(4)	Mn–CO$_{av.}$	1.846
CO$_{av.}$(Mn)	1.139	C(1)–C(2)	1.486(6)
C(1)–H(1A)	1.124(40)	C(1)–H(1B)	0.913(44)
C(2)–O(1)	1.212(5)		
C–C–C(cp)$_{av.}$	107.99	CP–Fe–C(1)	118.94(13)
CP–Fe–C(16)	124.62(12)	CP–Fe–C(17)	124.66(14)
C(1)–Fe–C(16)	90.77(17)	C(1)–Fe–C(17)	94.68(18)
C(16)–Fe–C(17)	94.65(18)	Fe–C(16)–O(11)	175.86(31)
Fe–C(17)–O(12)	175.25(35)	C(25)–Mn–C(21—24)$_{av.}$	93.75
C(21)–Mn–C(22)	90.11(19)	C(21)–Mn–C(24)	89.41(19)
C(22)–Mn–C(23)	89.62(19)	C(23)–Mn–C(24)	89.87(19)
C(2)–Mn–C(21—24)$_{av.}$	86.25	Mn–CO$_{av.}$	178.63
Fe–C(1)–C(2)	113.98(28)	Fe–C(1)–H(1A)	106.31(202)
Fe–C(1)–H(1B)	104.24(265)	C(2)–C(1)–H(1A)	103.68(216)
C(2)–C(1)–H(1B)	118.88(279)	H(1A)–C(1)–H(1B)	109.14(339)
C(1)–C(2)–Mn	119.56(28)	C(1)–C(2)–O(1)	122.00(35)
Mn–C(2)–O(1)	118.41(31)		

from the spectroscopic studies there is no interaction between the two metal centres linked by the ketene bridge. The metal–metal distances are 4.148(1) Å for (**1**) and 4.710(1) Å for (**2**). The structure of the Fe(cp)(CO)$_2$ parts (three-legged piano stool) is essentially the same as those of corresponding alkyl complexes[6] and of [{Fe(cp)(CO)$_2$}$_2$CH$_2$CO] (**3**).[7] The geometry of the Ni(cp)(CO) part in (**1**) shows very close similarities to that in [(OC)(cp)Ni–Mn(CO)$_5$][8] and to the Fe(cp)(CO)$_2$ group except for the number of carbonyl ligands. To our knowledge this is the first structure determination of a Ni(cp)(CO) complex containing an organic ligand. The Mn atom in (**2**) is surrounded by five carbonyls and the μ-ketene ligand, resulting in an octahedral co-ordination.[9]

Table 6. Structural parameters of bridging ketene ligands

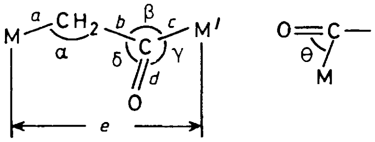

Complex	a	b	c	d	e	α	β	γ	δ	θ	ν(C=O)
(**1**) $[(OC)_2(cp)Fe(CH_2CO)Ni(cp)(CO)]$	2.088	1.482	1.940	1.205	4.148	111.9	117.3	118.0	124.6	88	1 649
(**2**) $[(OC)_2(cp)Fe(CH_2CO)Mn(CO)_5]$	2.082	1.486	2.173	1.212	4.710	114.0	119.6	118.4	122.0	64	1 581
(**3**) $[\{Fe(cp)(CO)_2\}_2CH_2CO]$	2.073	1.481	2.008	1.219	4.450	114.0	117.1	120.9	121.6	76	1 612
(**4**) $[Os_3(CO)_{12}(\mu\text{-}CH_2CO)]$	2.22	1.47	2.16	1.26	4.259	112.2	121.4	120.6	117.9	97	1 573
(**5**) $[Ru_2(\eta^5\text{-}C_5Me_5)_2(CO)_3(\mu\text{-}CH_2CO)]$	2.194	1.450	2.105	1.213	2.814	89.0	107.6			55	1 568
(**6**) $[\{Fe(cp)(CO)_2\}_2CH_2CH_2CO]$*	2.071	1.534	1.991	1.203	5.682	114.6	117.4	122.3	120.2	79	1 645

a—*e* in Å, α—δ in °, ν(C=O) in cm^{-1}. * CH_2–CH_2CO 1.519 Å, CH_2–C–CO 110.87°.

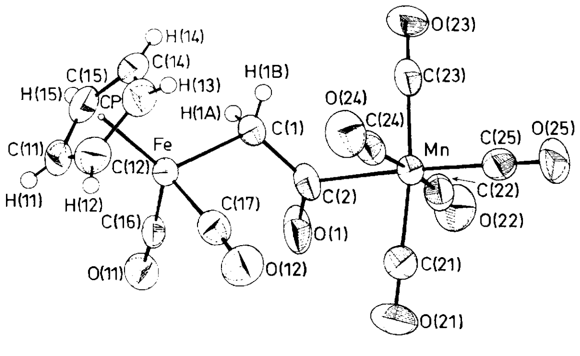

Figure 2. Molecular structure of $[(OC)_2(cp)Fe(CH_2CO)Mn(CO)_5]$ (**2**) showing 50% probability thermal ellipsoids

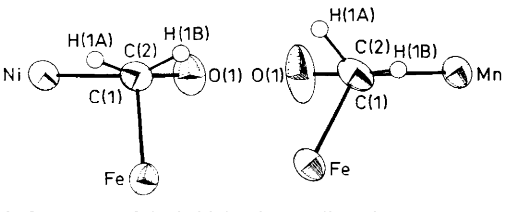

Figure 3. Geometry of the bridging ketene ligand

The structural parameters associated with the bridging ketene ligands accompanied by previously reported data[10,11] are listed in Table 6. Bond lengths and bond angles for C(1) and C(2) atoms fall in the range of those for sp^3- and sp^2-hybridized carbon atoms, respectively. To be noted is that the C(1)–C(2) bond lengths (*b*) are substantially shorter than the CH_2–CO bond length in complex (**6**) for which no contribution from a resonance form corresponding to (**C**) is detectable by spectroscopic methods. Therefore, the observed change in *b* should be attributed to the π-complex form (**C**) in which the C–C bond length is shortened owing to the increased double-bond character. In addition, the dihedral angle (θ) between the M–CH_2 and C=O planes in complex (**1**) (Figure 3) is almost a right angle. This conformation maximizes the overlap between the electron-diffusing Fe–CH_2 bond and the electron-deficient *p* orbital on the C(2) atom which projects perpendicular to the C=O bond. Similar results have been reported for μ-η^2-(C,C)-ketene complexes (3) and (4),[10] although some deviations in θ are observed for μ-ketene complexes with a bulky metal part, (2), and with a cyclic structure, (5).[11] The Fe–CH_2 bond lengths (*a*) are almost identical irrespective of the acyl-metal groups. On the other hand, the bond length *c* varies depending upon the radius of the metal atom. The Mn–C(2) distance (*c*) is significantly longer than those reported for CH_3COCO–$Mn(CO)_5$ (2.075 Å)[9] and CF_3CF_2CO–$Mn(CO)_5$ (2.047 Å).[12] No systematic relationship between the length *d* and the stretching vibration of the acyl C=O bond has been detected as shown in Table 6. While according to the extended Hückel molecular-orbital calculation by Hoffmann[13] the 'upright' and 'bisecting' conformations are predicted for olefin and carbene ligands, respectively, the conformations around the metal–carbon bonds do not reflect the resonance forms (**B**) (with carbene complex character) and (**C**) (with olefin complex character) but are apparently determined by non-bonding steric repulsions between the bridging ketene ligand and the ancillary ligands. With regard to the conformations around the Fe–C(1) bonds, CPFE (centroid of C_5H_5 group) and C(2) in (**1**) [with a less bulky Ni(cp)(CO) group] are located in a gauche-staggered conformation [CPFE–Fe–C(1)–C(2) 59.42°], while an anti-periplanar conformation is observed for (**2**) [with a more bulky $Mn(CO)_5$ group]. (For an ideal upright conformation the dihedral angle should be 90°.) As to the conformations around the M–C=O bonds, the acyl C=O bond is located parallel to the cp plane in (**1**) [CPNI–Ni–C(2)–C(1) 81.82°] and in a staggered conformation in (**2**) [C(23)–Mn–C(2)–C(1) 46.74°]. [For an ideal bisecting conformation the dihedral angle in (**1**) should be 180°.] Thus, the orbital interaction between the metal centre and the bridging ketene is too small to determine the conformations.

Consequently, the structure determinations by *X*-ray diffraction studies as well as the previously reported spectroscopic studies reveal that the geometry around the C–C bond of the bridging ketene ligand is determined by the π-complex resonance form (**C**) which is generally observed for polymetallic μ-η^2-(C,C)-ketene complexes, and that the co-operative metal-to-ligand back donation doubly activates the ketene ligand as a nucleophile.[1b,c,3,14]

Acknowledgements

We are grateful to the Asahi Glass Foundation for Industrial Technology and the Ministry of Science, Culture, and Education for financial support of this research.

References

1 (*a*) M. Akita, A. Kondoh, and Y. Moro-oka, *J. Chem. Soc., Chem. Commun.*, 1986, 1296; (*b*) M. Akita, A. Kondoh, T. Kawahara, and Y. Moro-oka, *J. Organomet. Chem.*, 1987, **323**, C43; (*c*) M. Akita, T. Kawahara, and Y. Moro-oka, *J. Chem. Soc., Chem. Commun.*, 1987,

1356; (*d*) M. Akita, A. Kondoh, T. Kawahara, T. Takagi, and Y. Moro-oka, *Organometallics*, 1988, **7**, 366.
2 G. L. Geoffroy and S. L. Bassner, *Adv. Organomet. Chem.*, 1988, **28**, 1 and refs. therein.
3 S. L. Bassner, E. D. Morrison, and G. L. Geoffroy, *Organometallics*, 1987, **6**, 2207.
4 J. K. P. Ariyaratne, A. M. Bierrum, M. L. H. Green, M. Ishaq, C. K. Prout, and M. G. Swanwick, *J. Chem. Soc. A*, 1969, 1309.
5 'International Tables for *X*-Ray Crystallography,' Kynoch Press, Birmingham, 1974, vol. 4.
6 See for example, L. Pope, P. Sommerville, and J. Laing, *J. Organomet. Chem.*, 1976, **112**, 309.
7 M. Akita, A. Kondoh, and Y. Moro-oka, *J. Chem. Soc., Dalton Trans.*, 1989, 1083.
8 T. Madach, K. Fischer, and H. Vahrenkamp, *Chem. Ber.*, 1980, **113**, 3235.
9 C. P. Casey, C. A. Bunnell, and J. C. Calabrese, *J. Am. Chem. Soc.*, 1976, **98**, 1166.
10 E. D. Morrison, G. R. Steinmetz, G. L. Geoffroy, W. C. Fultz, and A. L. Rheingold, *J. Am. Chem. Soc.*, 1984, **106**, 4783.
11 N. M. Doherty, M. J. Fildes, N. J. Forrow, S. A. R. Knox, K. A. Macpherson, and A. G. Orpen, *J. Chem. Soc., Chem. Commun.*, 1986, 1355.
12 M. R. Churchill, *Perspect. Struct. Chem.*, 1970, **3**, 126.
13 B. E. R. Schilling, R. Hoffmann, and D. L. Lichtenberger, *J. Am. Chem. Soc.*, 1979, **101**, 585.
14 M. Akita, T. Kawahara, M. Terada, and Y. Moro-oka, *Organometallics*, 1989, **8**, 687.

Received 14*th November* 1988; *Paper* 8/04513E